Supporting information

Molecular engineering of Ga-ketoiminates: Synthesis, structure and evaluation as precursors for the additive-free spin-coated deposition of gallium oxide thin films

Richard O'Donoghue,[a] Shafiqur Rahman,[a] Bert Mallick,[a] Manuela Winter,[a] Detlef Rogalla,[b] Hans-Werner Becker[b] and Anjana Devi[a]*

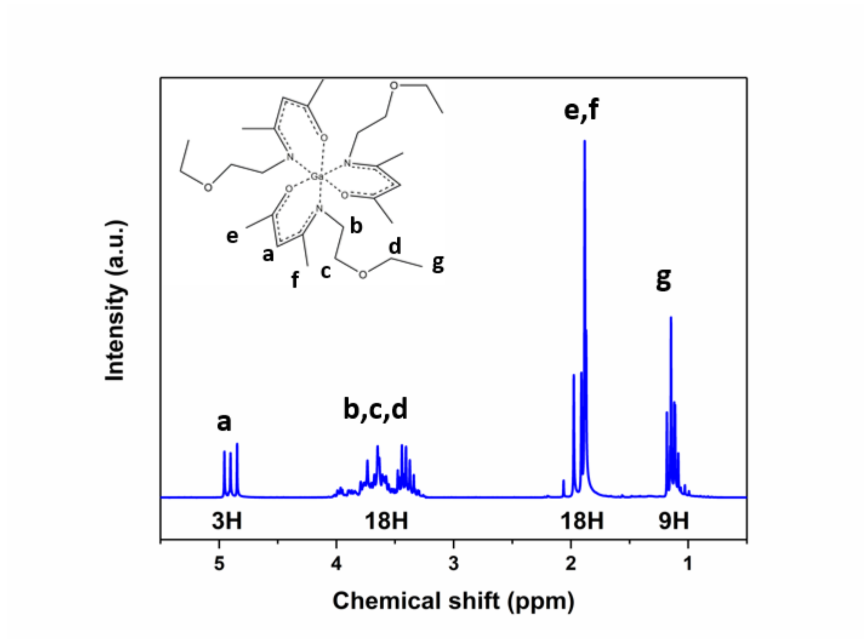

Figure S1. ^{1}H NMR spectrum of compound [**1**] – [Ga(eeki)$_3$].

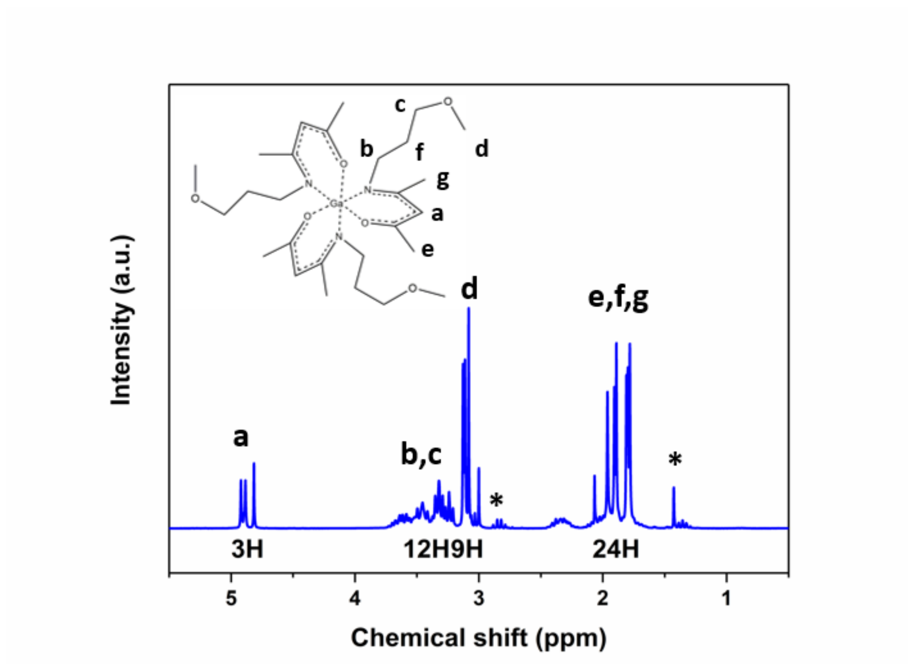

Figure S2. ^{1}H NMR spectrum of compound [**2**] – [Ga(mpki)$_3$]. * = Ligand.

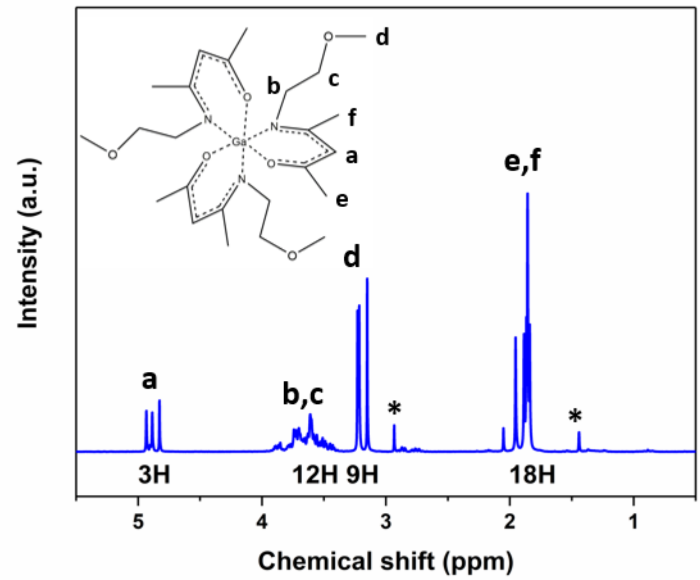

Figure S3. [1]H NMR spectrum of compound [**3**] – [Ga(meki)$_3$]. * = Ligand.

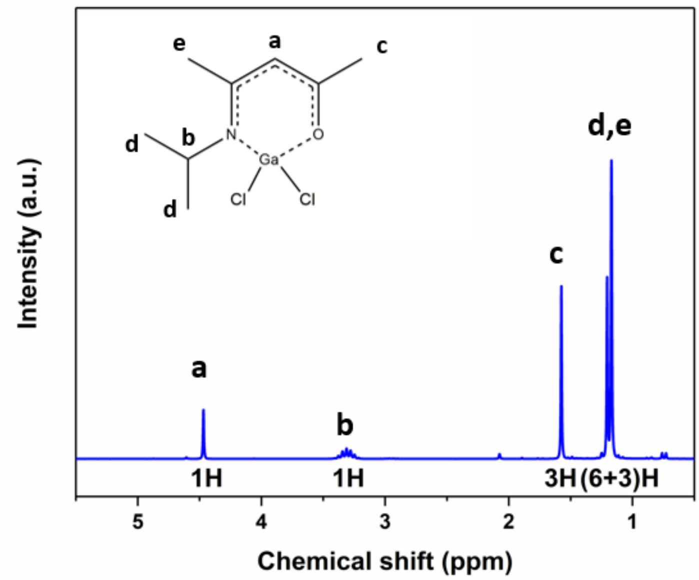

Figure S4. [1]H NMR spectrum of compound [**4**] – [Ga(ipki)Cl$_2$].

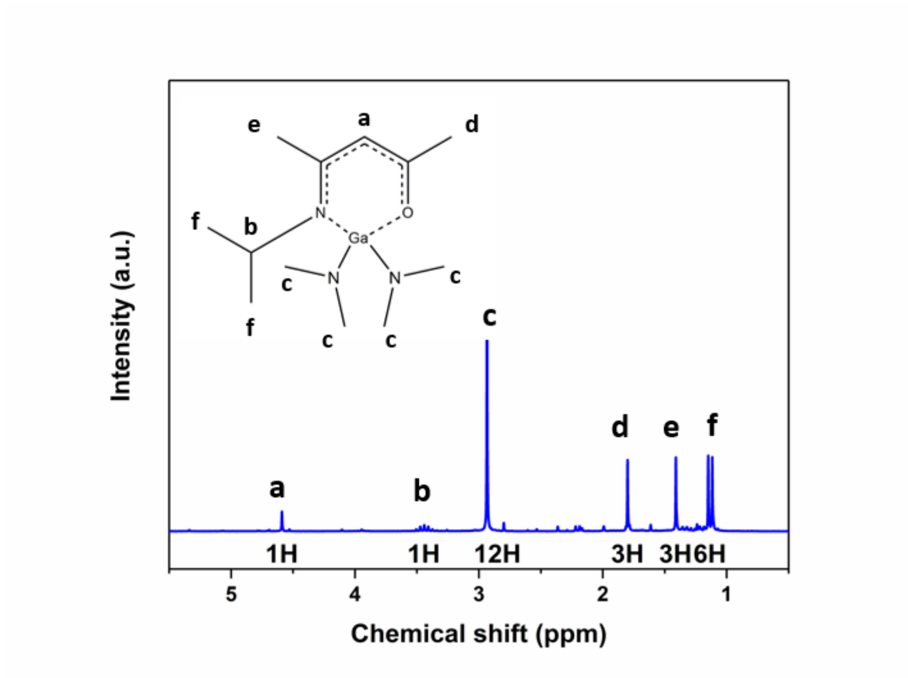

Figure S5. ^{1}H NMR spectrum of compound [**5**] – [Ga(ipki)$(NMe_2)_2$].

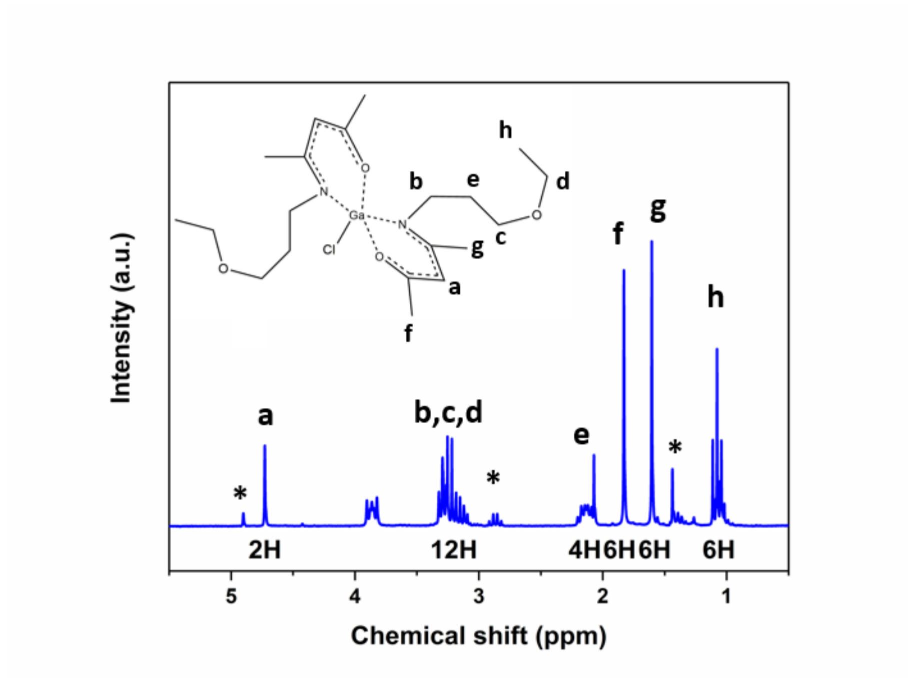

Figure S6. ^{1}H NMR spectrum of compound [**6**] – [Ga(epki)Cl_2]. * = Ligand.

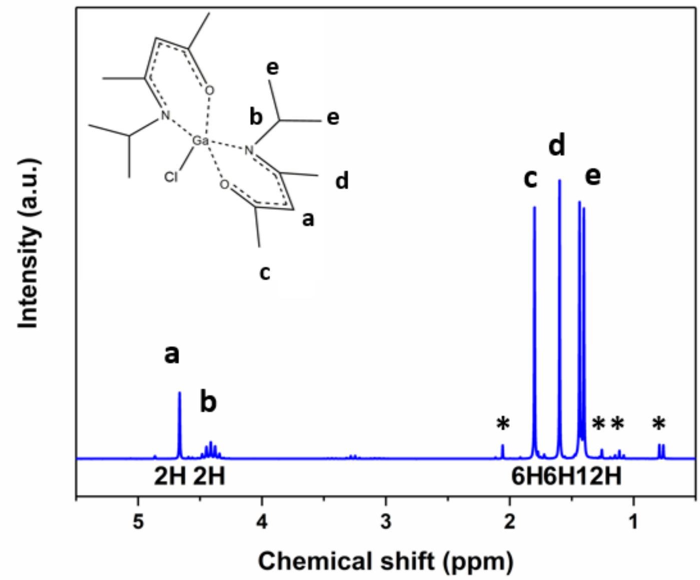

Figure S7. ^{1}H NMR spectrum of compound [**7**] – [Ga(ipki)$_2$Cl].* = Ligand

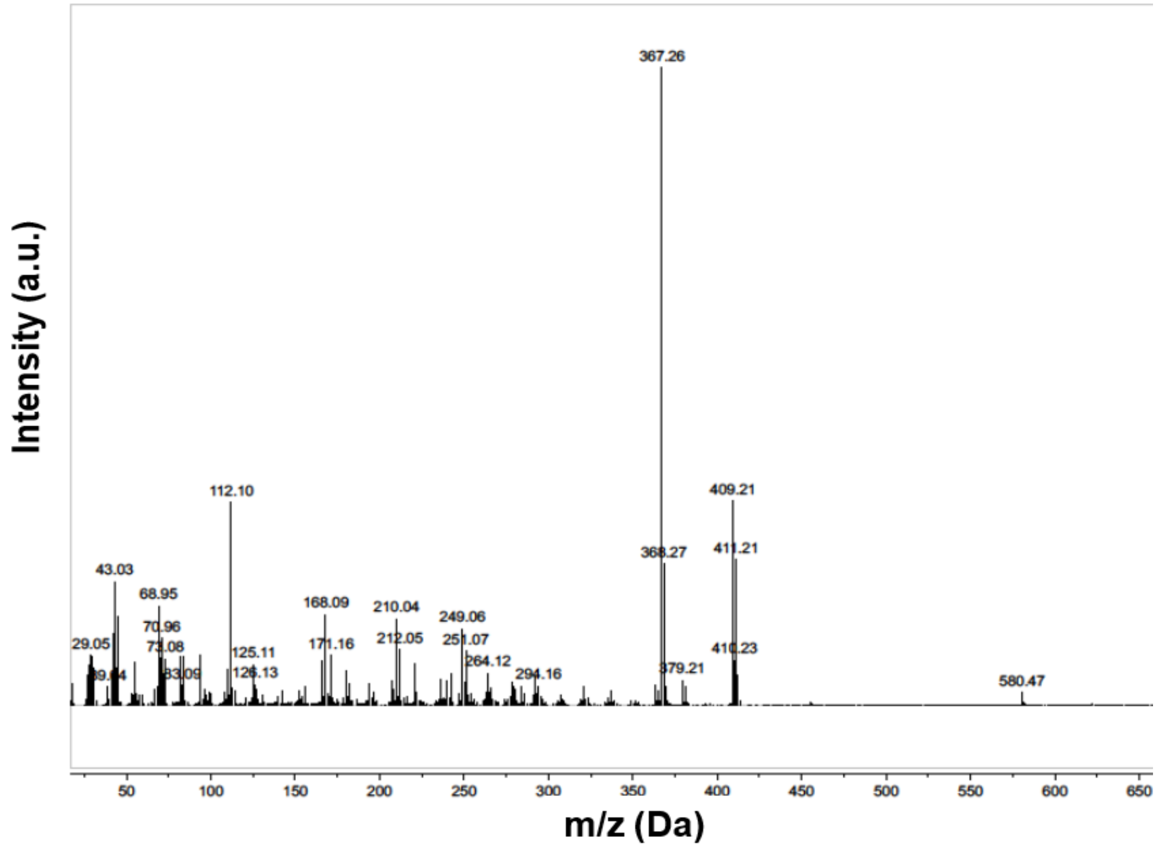

Figure S8. EI-MS spectrum of compound [**1**].

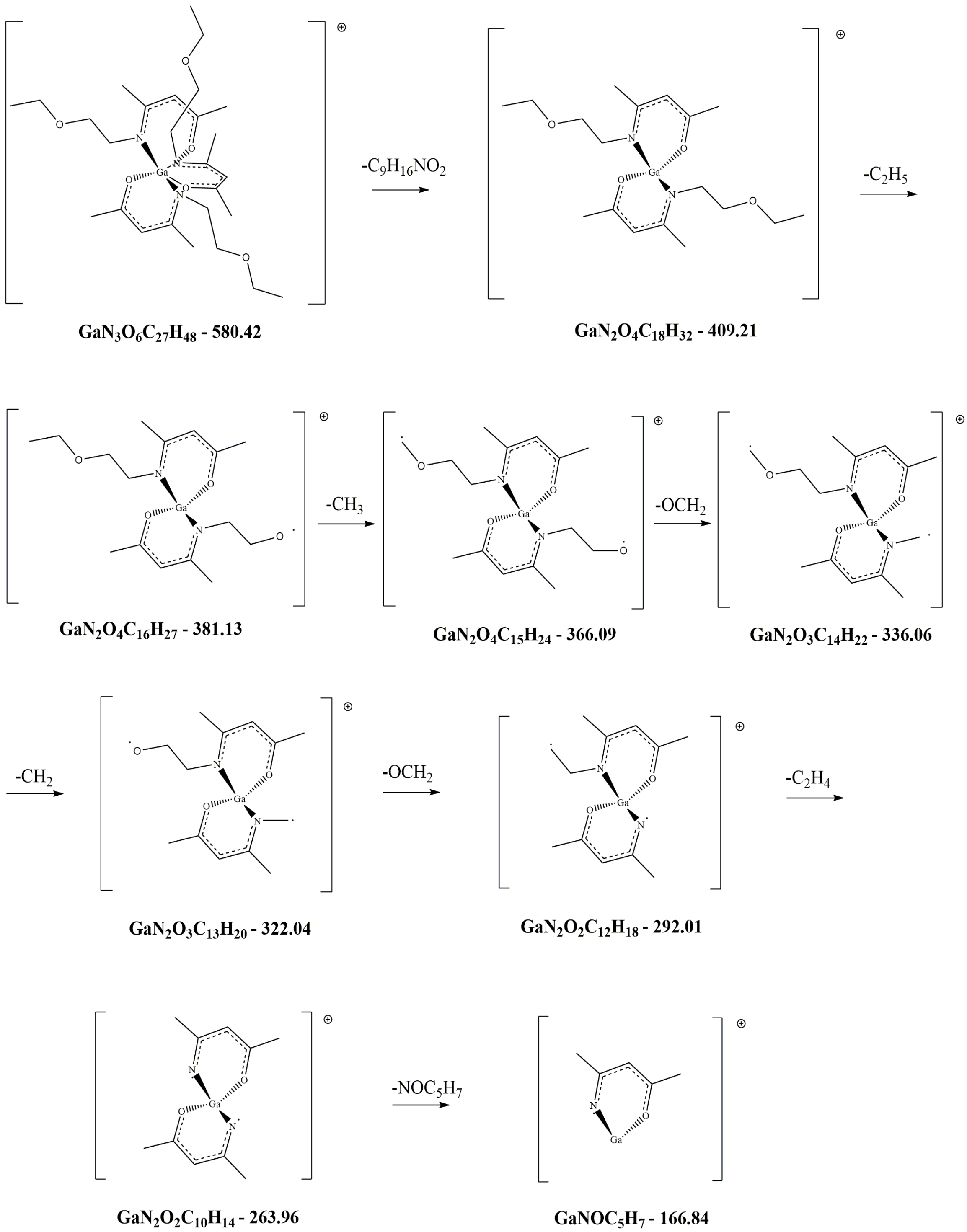

Figure S9. Proposed fragmentation pattern for the EI-MS data in Figure S2

Table S1. Overview of the fragments observed in the EI-MS spectra of compound [**4**].

Fragments	m / z	Intensity [%]
$[M^{+\cdot}]$	281.0	17.65
$[M^{+\cdot} - {}^{\cdot}CH_3]$	264.0	100.00
$[M^{+\cdot} - {}^{\cdot}Cl]$	244.0	54.99
$[M^{+\cdot} - {}^{\cdot}CH_3 - {}^{\cdot}Cl]$	228.0	71.23
$[M^{+\cdot} - {}^{\cdot}CH(CH_3)_2 - {}^{\cdot}CH_3]$	186.0	9.03
$[Ligand^{+\cdot}]$	140.9	18.66
$[M^{+\cdot}$ - 1x Ligand]	138.9	13.71
$[Ga^{+\cdot}]$	68.9	15.18
$[H_2CCHCH_3{}^{+\cdot}]$	42.0	44.92
$[H_2CCH^{+\cdot}]$	27.0	14.06

Table S2. Overview of the fragments observed in the EI-MS spectra of compound [**5**].

Fragments	m / z	Intensity [%]
$[M^{+\cdot}]$	298.2	1.53
$[M^{+\cdot} - {}^{\cdot}N(CH_3)_2]$	253.1	78.75
$[M^{+\cdot} - {}^{\cdot}- {}^{\cdot}2N(CH_3)_2]$	209.3	47.40
$[M^{+\cdot} - {}^{\cdot}2N(CH_3)_2 - {}^{\cdot}2CH_3]$	166.0	1.53
$[Ligand^{+\cdot}]$	140.1	0.78
$[Ligand^{+\cdot} - {}^{\cdot}CH_3]$	108.1	7.59
$[Ligand^{+\cdot}$ - 2x $^{\cdot}CH_3]$	83.1	7.33
$[Ga^{+\cdot}]$	68.9	48.22
$[H_2CCHCH_3{}^{+\cdot}]$	42.0	100.00
$[H_2CCH^{+\cdot}]$	27.0	12.04

Table S3. Overview of the fragments observed in the EI-MS spectra of compound [**6**].

Fragments	m / z	Intensity [%]
$[M^{+\cdot}]$	474.2	1.21
$[M^{+\cdot} - {}^{\cdot}Cl]$	439.2	64.74
$[M^{+\cdot} - {}^{\cdot}Cl - {}^{\cdot}OCH_2CH_3]$	395.2	21.46
$[M^{+\cdot} - {}^{\cdot}Cl - {}^{\cdot}2CH_2CH_2OCH_2CH_3]$	292.1	6.53
$[M^{+\cdot} - {}^{\cdot}Cl - {}^{\cdot}2CH_2CH_2OCH_2CH_3 - {}^{\cdot}4CH_3]$	223.1	2.55
$[Ligand^{+\cdot}]$	186.2	18.42
$[Ga^{+\cdot}]$	68.9	3.20
$[H_2CCHCH_3{}^{+\cdot}]$	42.0	7.80
$[H_2CCH^{+\cdot}]$	27.0	4.41

Table S4. Overview of the fragments observed in the EI-MS spectra of compound [**7**].

Fragments	m / z	Intensity [%]
$[M^{+\cdot}]$	384.2	26.70
$[M^{+\cdot} - {}^{\cdot}CH_3]$	371.1	21.46
$[M^{+\cdot} - {}^{\cdot}Cl]$	349.2	90.83
$[M^{+\cdot} - {}^{\cdot}Cl - 4x\ {}^{\cdot}CH_3]$	291.1	13.66
$[M^{+\cdot} - {}^{\cdot}Cl - 3x\ {}^{\cdot}CH_3 - {}^{\cdot}CH(CH_3)_2]$	264.1	26.77
$[M^{+\cdot} - {}^{\cdot}Cl - 4x\ {}^{\cdot}CH_3 - {}^{\cdot}CH(CH_3)_2]$	249.1	22.47
$[M^{+\cdot}$ - 1x Ligand$]$	244.0	100.00
$[M^{+\cdot}$ - 1x Ligand - ${}^{\cdot}CH_3]$	228.0	18.54
$[M^{+\cdot}$ - 1x Ligand - ${}^{\cdot}OCCH_3]$	202.0	35.37
[Ligand$^{+\cdot}$]	140.1	68.12
[Ligand$^{+\cdot}$ - ${}^{\cdot}CH_3$]	126.1	23.61
[Ligand$^{+\cdot}$ - 2x ${}^{\cdot}CH_3$]	108.1	18.36
[Ligand$^{+\cdot}$ - ${}^{\cdot}CH_3$ - ${}^{\cdot}CH(CH_3)_2$]	83.1	24.84
$[Ga^{+\cdot}]$	68.9	33.00
$[H_2CCHCH_3^{+\cdot}]$	42.0	73.07
$[H_2CCH^{+\cdot}]$	27.0	21.51

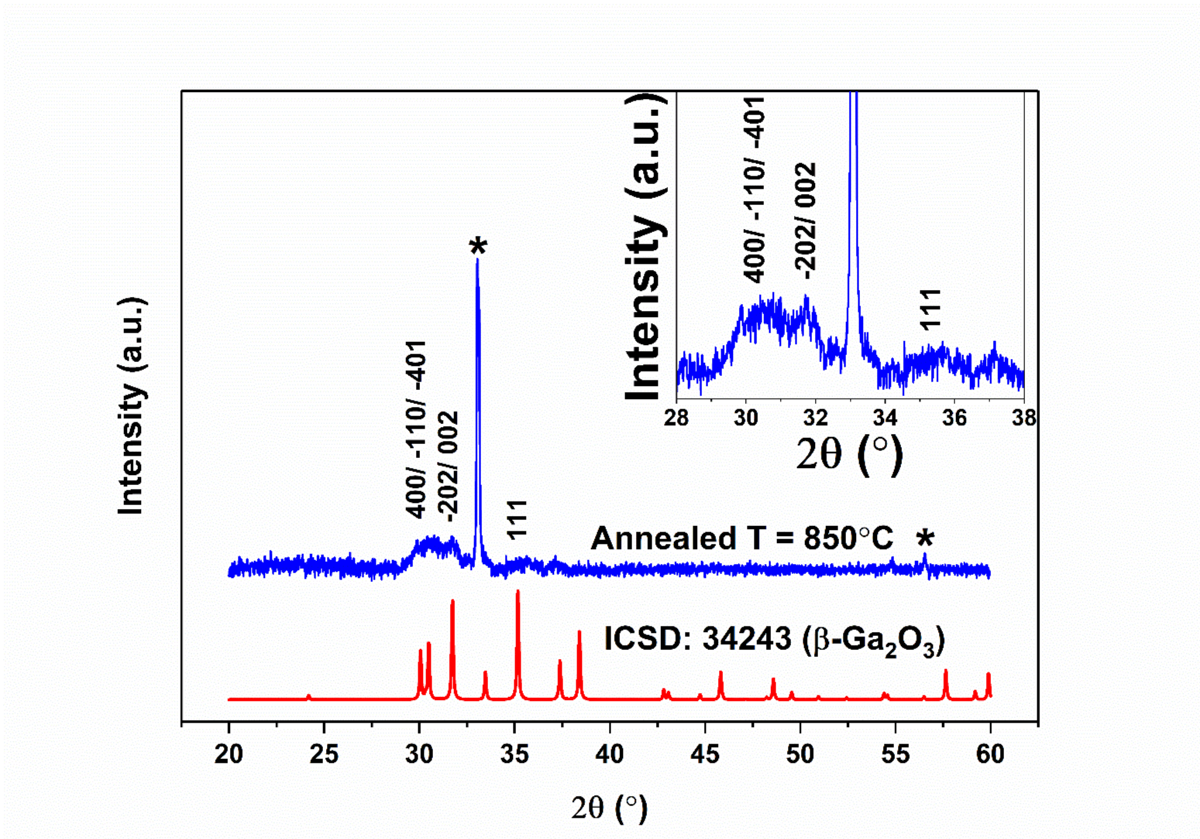

Figure S10. XRD pattern of the gallium oxide thin film from a process deposited on Si(100) using compound [**1**] with 25 spin coating cycles at a hotplate temperature of 350 °C after annealing at 850 °C for 2 h under ambient conditions. The β-gallium oxide reference pattern in red corresponds to the ICSD no. 34243. The Inset shows a close up of the obtained reflexes.* = silicon substrate.

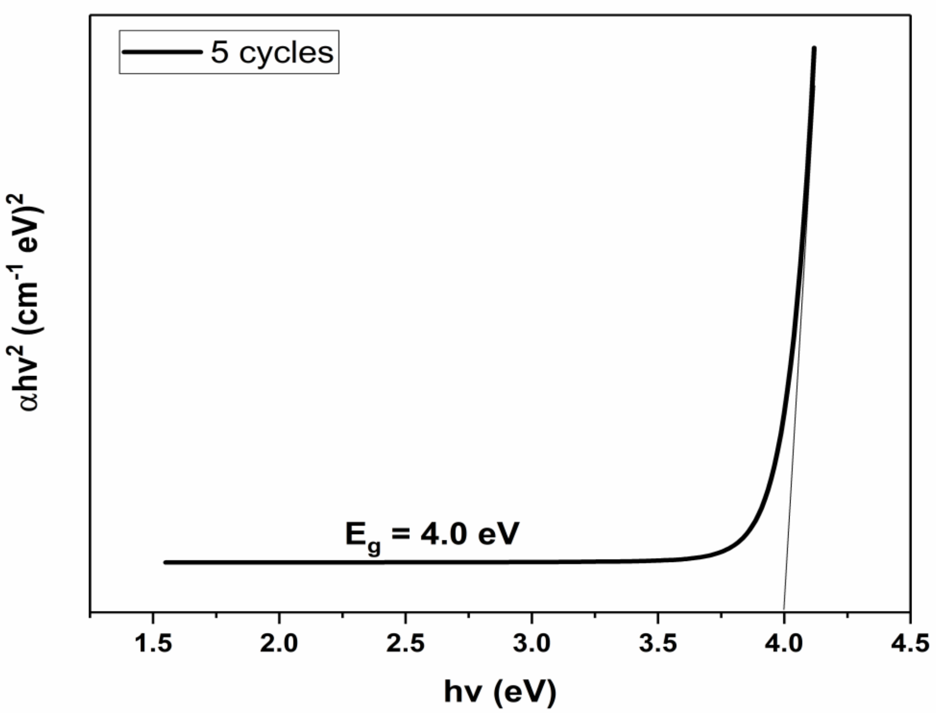

Figure S11. Tauc plot derived from the transmittance data of the sample deposited with 5 spin-cycles.

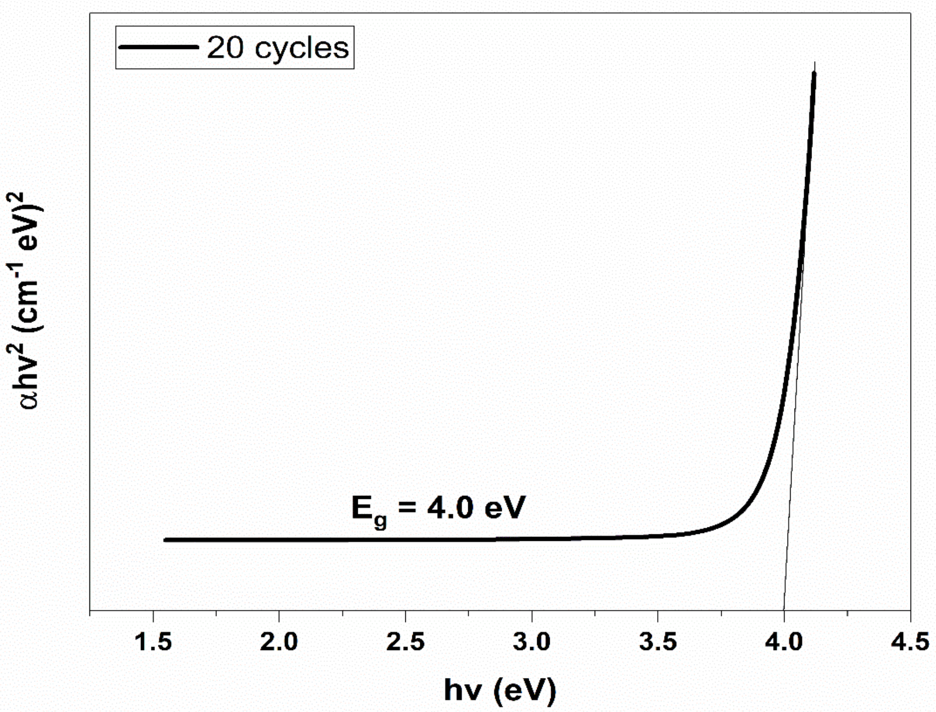

Figure S12. Tauc plot derived from the transmittance data of the sample deposited with 20 spin-cycles.

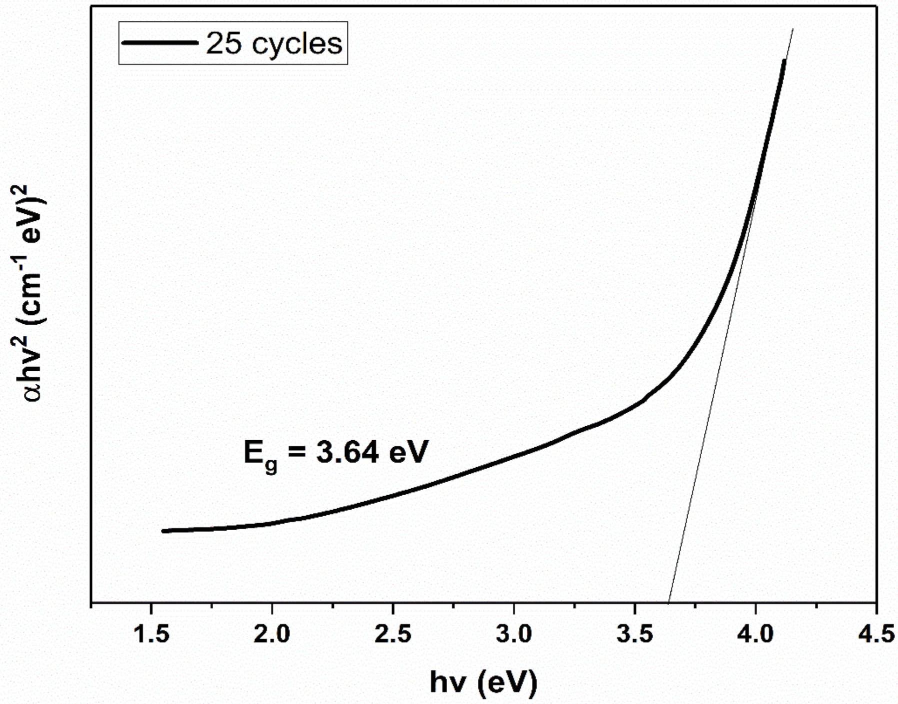

Figure S13. Tauc plot derived from the transmittance data of the sample deposited with 25 spin-cycles